

RESEARCH

Open Access



A comprehensive transcriptional reference for severity and progression in spinal cord injury reveals novel translational biomarker genes

Rubén Grillo-Risco¹, Marta R. Hidalgo^{1,2}, Beatriz Martínez-Rojas³, Victoria Moreno-Manzano^{3*} and Francisco García-García^{1*} 

Abstract

Spinal cord injury (SCI) is a devastating condition that leads to motor, sensory, and autonomic dysfunction. Current therapeutic options remain limited, emphasizing the need for a comprehensive understanding of the underlying SCI-associated molecular mechanisms. This study characterized distinct SCI phases and severities at the gene and functional levels, focusing on biomarker gene identification. Our approach involved a systematic review, individual transcriptomic analysis, gene meta-analysis, and functional characterization. We compiled a total of fourteen studies with 273 samples, leading to the identification of severity- and phase-specific biomarker genes that allow the precise classification of transcriptomic profiles. We investigated the potential transferability of severity-specific biomarkers and identified a twelve-gene signature that predicted injury prognosis from human blood samples. We also report the development of MetaSCI-app - an interactive web application designed for researchers - that allows the exploration and visualization of all generated results (<https://metasci-cbl.shinyapps.io/metaSCI>). Overall, we present a transcriptomic reference and provide a comprehensive framework for assessing SCI considering severity and time perspectives, all integrated into a user-friendly tool.

Introduction

Spinal cord injury (SCI) leads to alterations in the motor, sensory, and autonomic systems immediately below the affected spinal segment, which represent a devastating blow to patients' quality of life due to the loss of voluntary movement and associated physiological dysfunction [1–3]. The World Health Organization (WHO) estimates

that 250,000–500,000 people suffer from SCI each year. Sadly, we currently lack a cure for SCI, although substantial efforts support a wide range of preclinical research aims [4, 5]. A recent reports from the Courtine lab have defined a neuronal subpopulation responsible for functional regeneration after epidural electrical stimulation in mice [6]; nevertheless, we still require concerted efforts in basic research to elucidate the dynamic, complex molecular mechanisms that underlie the distinct stages of SCI. Likewise, an improved understanding of the mechanisms at play (and their biological relevance) in the early stages after SCI is needed to control evolution in acute cases and achieve functional recovery in those patients suffering from chronic injuries.

*Correspondence:

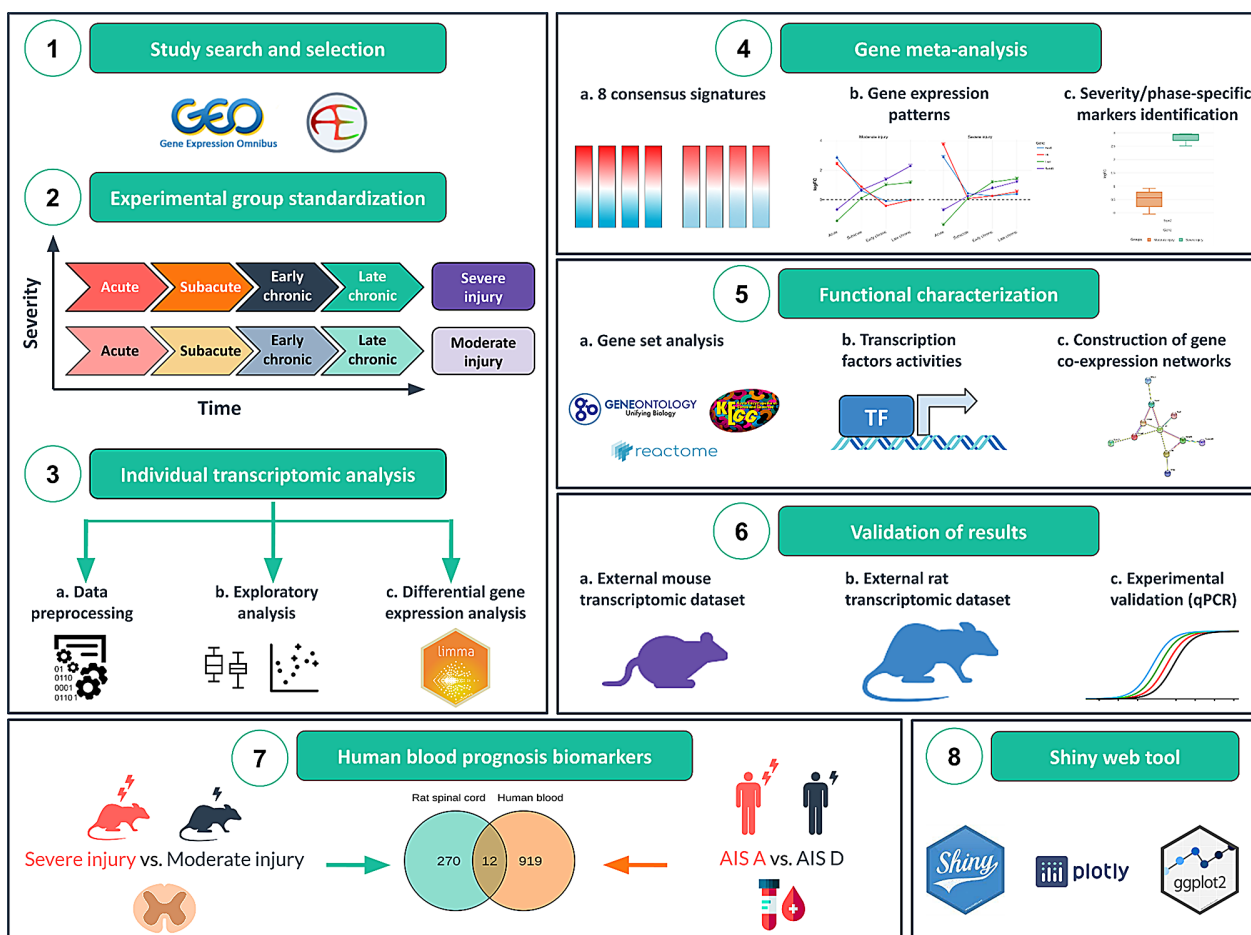
Victoria Moreno-Manzano
vmorenom@cipf.es
Francisco García-García
fgarcia@cipf.es

Full list of author information is available at the end of the article



© The Author(s) 2024. **Open Access** This article is licensed under a Creative Commons Attribution-NonCommercial-NoDerivatives 4.0 International License, which permits any non-commercial use, sharing, distribution and reproduction in any medium or format, as long as you give appropriate credit to the original author(s) and the source, provide a link to the Creative Commons licence, and indicate if you modified the licensed material. You do not have permission under this licence to share adapted material derived from this article or parts of it. The images or other third party material in this article are included in the article's Creative Commons licence, unless indicated otherwise in a credit line to the material. If material is not included in the article's Creative Commons licence and your intended use is not permitted by statutory regulation or exceeds the permitted use, you will need to obtain permission directly from the copyright holder. To view a copy of this licence, visit <http://creativecommons.org/licenses/by-nc-nd/4.0/>.

Graphical abstract



Keywords Spinal cord injury, Transcriptomics, Meta-analysis, Biomarkers, Functional profiling, Translational, Prognosis

Transcriptomics represents a widely used technology for the study of pathological states such as SCI; this technique provides a comprehensive view of the cellular responses to a given condition from a systems biology perspective and allows the identification of differentially expressed genes (DEGs). Unfortunately, statistically significant DEGs from studies can display distressingly little overlap when distinct research groups study the same biological system [7]. This lack of robustness and reproducibility can lead to conflicting or inconclusive results. Although many transcriptomic studies of SCI exist, we still lack consensus regarding the description of the injury-induced transcriptomic profile and its functional correlation, which hinders the identification of therapeutic targets with sufficient depth over time and based on injury severity due to heterogeneity between injuries/models.

To solve such issues, we propose a novel characterization of SCI through a meta-analysis of transcriptomic

studies. A meta-analysis represents an integrative approach that allows for a more precise measurement of the effect of interest than individual studies, thus increasing statistical power, and considers the variability of individual studies to provide more consistent results [8]. We based our strategy on the systematic review and selection of public transcriptomic studies performed in rats since 2004. We grouped samples based on severity and time after injury, allowing the characterization of SCI in two dimensions. We subsequently processed and analyzed all datasets similarly to avoid introducing biases associated with bioinformatics pipelines [9]. We performed a gene expression meta-analysis to integrate individual differential gene expression (DGE) analysis results, providing a consensus gene expression signature for each group. We identified specific severity- and phase-associated biomarker genes from the generated gene expression patterns. We then functionally characterized these transcriptomic profiles to estimate the dysregulated

pathways, infer transcription factor (TF) activity, and construct gene co-expression networks. We bioinformatically validated the results with two external datasets and experimentally by quantitative (q-)PCR. We also explored the potential transferability of severity-specific biomarker genes found in rats to predict injury prognosis in human blood samples. Finally, we created the Meta-SCI app, a platform that allows the research community to access and deeply explore all generated results.

Results

Identifying gene consensus signatures based on severity and time

We first performed a systematic review and selection of studies in GEO [10] and ArrayExpress [11] databases following the Preferred Reporting Items for Systematic Reviews and Meta-Analyses (PRISMA) guidelines [12]. After applying inclusion and exclusion criteria, we finally selected 14 studies and 273 samples for our meta-analysis (Fig. S1; Table S1). Given the diversity of studies, we standardized metadata to create experimental groups with uniform nomenclature. We categorized injury severity into moderate (M) and severe (S) groups (Table S2). We established four injury phase groups based on time after injury and sample collection: acute (0–3 days, T1), subacute (4–14 days, T2), early chronic (15–35 days, T3), and late chronic (> 35 days, T4) [3, 13, 14]. Controls comprised samples from sham-operated or non-operated naïve rats. Table S3 reports sample identifiers and annotations, while Table S4 and Fig. S2 detail sample distribution into the distinct experimental groups.

We followed a common pipeline that included data preprocessing, exploratory analysis, and DGE analysis for the individual analysis of the selected datasets. Since we aimed to characterize SCI in all phases and analyze the influence of injury severity, we compared each injury group against the control group within their study to identify DEGs. The eight comparisons performed and the abbreviations used for simplicity are: M1 (Moderate Acute [T1] vs. Control), M2 (Moderate Subacute [T2] vs. Control), M3 (Moderate Early chronic [T3] vs. Control), M4 (Moderate Late chronic [T4] vs. Control), S1 (Severe Acute [T1] vs. Control), S2 (Severe Subacute [T2] vs. Control), S3 (Severe Early chronic [T3] vs. Control), and S4 (Severe Late chronic [T4] vs. Control).

By conducting a meta-analysis, we integrated DGE analysis results for each comparison to obtain a transcriptional consensus signature for each experimental group. Fig. S3A reports the number of studies per group, while Fig. S3B displays the high number of significant genes (false discovery rate [FDR] < 0.05) in each comparison in our study. The “Individual analysis” and “Meta-analysis” modules of the Meta-SCI app contain a detailed list of all results.

We performed a principal component analysis (PCA) and hierarchical clustering analysis of transcriptional consensus signatures to generate an overview of similarities between groups. Together, we observed a separation between severe and moderate injuries, with similarities between M1 and S1, suggesting the acute phase as the most distinctive temporal phase irrespective of severity (Fig. 1A, B).

Identification of predictive biomarker genes for severity assessment

To identify severity-specific biomarker genes, we compared transcriptional consensus signatures of the four severe injury groups against the four moderate injury groups (Table S5), identifying 282 genes with an FDR < 0.1 (Table S6). Interestingly, the hierarchical heatmap revealed higher gene dysregulation (upregulated or downregulated) in severe compared to moderate injuries (Fig. S4), resulting in a clear separation of two distinct heatmap branches based on severity. Figure 1C, D illustrate that the top 10 most significantly altered genes (*Srpx2*, *Hoxb8*, *Acap1*, *Snai1*, *Aadat*, *Ppic*, *Lrrc17*, *Map7*, *Actg2*, and *H19*) enabled a clear separation between moderate and severe injuries, with PC1 explaining 93% of the variance in the PCA. The expression patterns of the top 5 severity-specific biomarker genes demonstrated consistent and more heightened dysregulation over time following severe injury (Fig. 1E), which represents a suitable pattern for injury prognosis.

We divided the list of 282 potential severity-specific genes into upregulated and downregulated genes and conducted a protein-protein interaction (PPI) analysis to evaluate functional relationships. The PPI network of downregulated genes (152) revealed enrichments in functions related to nervous system development and the regulation of trans-synaptic signaling (Fig. S5). Meanwhile, the PPI network of upregulated genes (130) exhibited enrichment in functions related to extracellular matrix organization, animal organ development, and anatomical structure morphogenesis (Fig. S6).

Effective group classification using phase-specific biomarker genes

To systematically identify phase-specific biomarker genes (independent of severity), we compared each phase against the remaining phases. Additionally, we investigated potential phase-specific biomarker genes for moderate and severe injury severity (Table S5). Table 1 reports the top 10 genes for each comparison. The acute phase displayed the most distinct transcriptional signature, with 770 genes encountered at FDR < 0.1; meanwhile, the other comparisons did not yield significant genes at this threshold. Nevertheless, using the top 10 genes with the

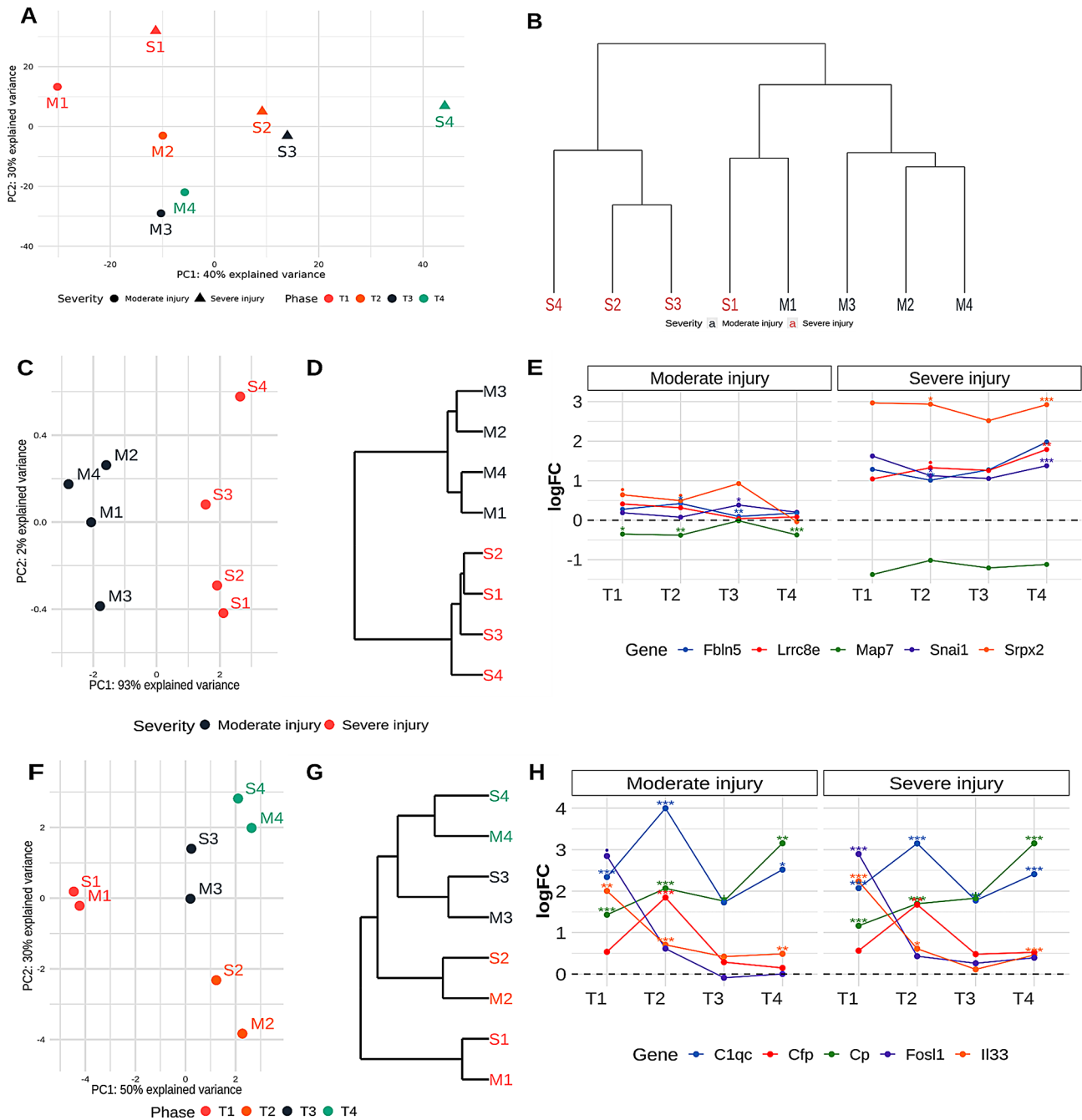


Fig. 1 Biomarker genes support effective group classification based on severity or phase after injury. **(A)** PCA plot and **(B)** hierarchical clustering of logFC gene consensus signatures for all groups. **(C)** PCA reveals a clear separation of groups based on injury severity using the top 10 severity-specific genes (93% of variance explained by PC1). **(D)** The hierarchical clustering of the top 10 genes highlights a clear branching pattern that effectively segregates groups based on severity. **(E)** Gene expression patterns of the top 5 severity-specific biomarkers. **(F)** PCA plot and **(G)** hierarchical clustering reveal a pairwise temporal classification of groups. **(H)** Gene expression patterns of a selection of different phase-specific genes - *Fosl1* and *Il13* as T1-specific; *C1qc* and *Cfp* as T2-specific; and *Cp* as T4-specific

lowest p-value in each case allowed clear group separation (Figs. S7–10 and Tables S7–10).

We selected the top 10 genes from the T1, T2, and T4 groups to create a phase-specific consensus signature, resulting in robust group separation (Fig. 1F, G). In the PCA plot (Fig. 1F), PC1 separated M1/S1 from the

remaining groups, while PC2 classified the remaining groups into pairs, with more similarity between M3/S3 and M4/S4, indicating that the selected biomarkers allow the identification of the injury phase independently of severity. Figure 1G depicts a similar segregation. While we identified the top 10 potential biomarker genes for T3

Table 1 Top 10 specific biomarker genes for each severity- and time-associated comparison

Comparison	Genes
Severity	SrpX2 , Hoxb8, Acap1 , Snai1 , Aadat, Ppic , Lrrc17 , Map7, Actg2 , H19
T1	Fosl1 , Il33 , Vcam1, Mx2, Mdk, Ldlr , Hmgcr , Alpk3, Dusp5 , Serpina3n
T2	Cfp , Slc46a3 , Scn8a, Ly86 , Casr , C1qc , Slc2a5 , Fgd2 , Aif1 , Slc7a7
T3	Slc28a2, Iqgap1, Cd14, Nt5dc2, Xdh, Msn, Lyve1, Tmem37, Rdh10, Enpp3
T4	Cp , Rab27a , Rab3b , Cybrd1 , Thrsp , Plcb1, Pmp22 , Acot2 , Cyp27a1 , RT1-Db1
M1	Hmgcs1 , Fdps , Cd68, Gpx2 , Alpk3, Crym , Apln , Slc15a2, Pltp, Ldlr
M2	Mmp8 , Cxcl13 , Cd8a , Casr , C1qb , RT1-CE4 , Fap , Cfp , Mmp7 , Slc7a7
M3	Sost , Rbp1, Cd14, Esm1, Hck, Plag1 , Fam102b , Atf3, Slc36a3 , Itgb8
M4	Thrsp , Ccl3, Tmem204 , Calml4 , Cpxm2 , Ckap2, Ttk, Csf3r, G0s2 , Mpz
S1	Fosl1 , Il6 , Kng2 , Tnfrsf12a , Upp1 , Myc , Gprc5a , C3, Exo1 , Chodl
S2	Apoc1 , Cfp , Tnr , Slc28a3 , C1qa , Slc46a3 , Casr , Postn , Slc40a1 , Pnlip
S3	Enpp3, Ccl4, Cd36, Lox, Igsf6, Xdh, Fcrl2, Msr1, Slc28a2, Rnf4
S4	Mmrn1 , Esm1 , Anxa8 , Crabp2 , Bnc2 , Igfbp6 , Slco2a1 , Ptgis , Tspan8 , Pde5a

Severity, (S1, S2, S3, S4) vs. (M1, M2, M3, M4); **T1**, (M1, S1) vs. (M2, M3, M4, S2, S3, S4); **T2**, (M2, S2) vs. (M1, M3, M4, S1, S3, S4); **T3**, (M3, S3) vs. (M1, M2, M4, S1, S2, S4); **T4**, (M4, S4) vs. (M1, M2, M3, S1, S3, S4); **M1**, M1 vs. (M2, M3, M4); **M2**, M2 vs. (M1, M3, M4); **M3**, M3 vs. (M1, M2, M4); **M4**, M4 vs. (M1, M2, M3); **S1**, S1 vs. (S2, S3, S4); **S2**, S2 vs. (S1, S3, S4); **S3**, S3 vs. (S1, S2, S4); **S4**, S4 vs. (S1, S2, S3). Genes in bold are upregulated in each comparison, while the others are downregulated

(demonstrating the segregation of M3/S3 from remaining groups), we do not consider them appropriate biomarkers (Fig. S8) as their characteristic expression pattern depicts a decrease between T2 and T4. This profile could be explained by a lack of consensus in results due to data heterogeneity rather than a genuine drop in gene expression during this phase. T3 likely represents a transitional phase between T2 and T4 without any expected expression biological process that peaks in T3, as one might anticipate in T2.

The PPI analysis with upregulated T1-specific genes revealed enrichment in responses to stress, cell cycle, and various metabolic processes (Fig. S11). Notably, upregulated genes demonstrated increased expression after injury that declined over time (as evidenced by gene expression patterns of *Fosl1* and *Il33* in Fig. 1H, for instance). We also detected genes such as *Lcat*, *Vcam1*, or *Fxyd1*, which become downregulated in T1 but upregulated in the following phases. Downregulated genes displayed enrichment for processes related to nervous system development and lipid metabolism (Fig. S12). Overall, these two divergent gene expression profiles represent valuable tools to distinguish T1 from the other stages. By utilizing the top 10 potential T1-specific genes, PCA1 effectively captures 95% of the variance, resulting in a distinct separation between M1/S1 and the remaining groups (Fig. S7). T2-specific genes displayed gene upregulation peaking in T2 that declined in subsequent phases; the *Cfp* and *C1qc* complement genes associated with secondary immune response [15, 16] exemplify this pattern (Fig. 1H). Potential T4-specific biomarker genes displayed increased expression from T1 that peaked in T4, as seen for *Cp* (ceruloplasmin) (Fig. 1H). For T2 and T4, the enrichment of the top 25 genes (arbitrary threshold) revealed immune response involvement in T2 (Fig. S13) and lipid metabolism enrichment in T4 (Fig. S14).

Overall, our meta-analysis allowed the successful identification of biomarker genes for each injury phase after SCI in independent studies with different rat models.

Functional characterization of gene consensus signatures

Next, we conducted three different analyses to characterize the gene consensus signatures obtained in the meta-analysis. First, we performed a functional enrichment analysis for each group via gene set analysis (GSA). Fig. S15A reports the number of significant functions (FDR < 0.05) grouped by database, severity, phase, and direction of enrichment. Venn diagrams for moderate and severe injury indicated a high number of shared functions between the four time phases for upregulated and downregulated functions (Fig. S15B), suggesting the existence of dysregulated mechanisms induced by the SCI that persist into chronic phases. We used Reactome annotation to classify significantly affected pathways to achieve an overview of the biological categories most affected after SCI (Fig. 2A). The immune system represents one of the most prevalent categories for significantly upregulated pathways in all comparisons independently of severity. These pathways form part of the core of permanent dysregulated pathways, which can be explained by the massive infiltration of inflammatory cells during the acute phase, the intrinsic microglial activation at the injury site, and a failure to efficiently resolve inflammation during the chronic stage [17]. In contrast, the elevated presence of pathways related to cell cycle, DNA repair, or DNA replication in the acute phase decreases over time, which could be explained by the proliferation of spinal cord resident cells such as microglia and macroglia (astrocytes and oligodendrocyte precursor cells) and infiltrating cells such as pericytes, fibroblasts or Schwann cells [18–21].

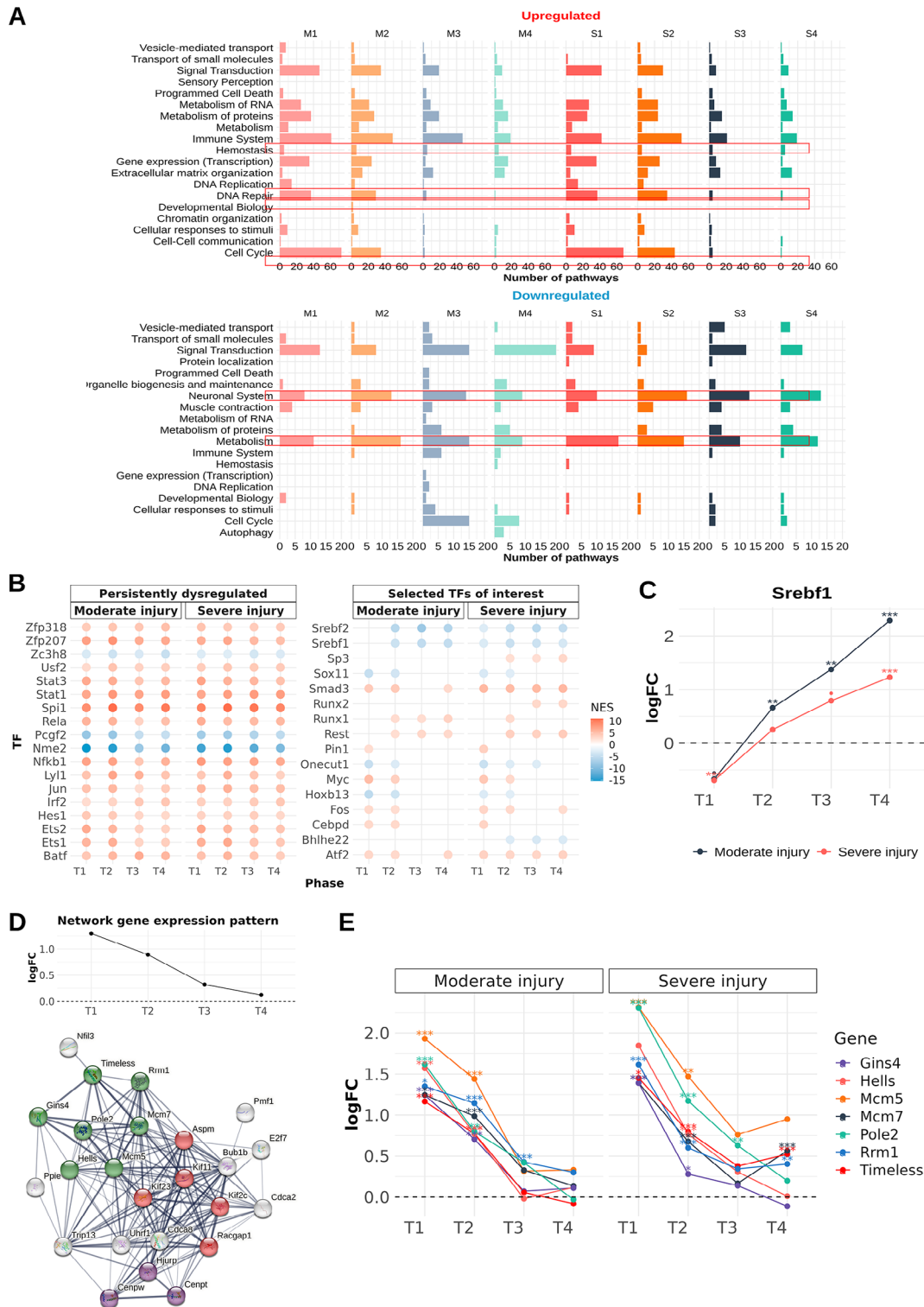


Fig. 2 Functional characterization reveals altered pathways and transcription factors across phase and severity after injury. **(A)** Frequency distribution of Reactome categories by phase and injury severity in upregulated and downregulated pathways. This value represents the sum of all significantly altered pathways within the same biological category in a comparison. Red squares highlight biological categories of interest. **(B)** Dotplot of significant dysregulated transcription factors (TFs) in all groups (left) and selected TFs of interest with significantly different activities (right) (Red – activation; blue – deactivation). **(C)** Gene expression patterns for *Srebf1*. **(D)** Moderate injury - cluster 11, subnetwork 1 - functionally relates to the cell cycle. All subnetwork proteins display a functional relationship and exhibit the same expression pattern. Red, green, and purple proteins form physical complexes among themselves. **(E)** Gene expression patterns of green proteins in moderate injury cluster 11, subnetwork 1

The permanent loss of neuronal system function and metabolism characterizes significantly downregulated pathways. Regarding metabolism-associated functions, the dotplot in Fig. S16 reports the downregulation of functions related to fatty acid synthesis, cholesterol synthesis, and the Krebs cycle in all groups, as previously described [22, 23].

Fig. S17 reports the downregulation of genes involved in cholesterol synthesis in a hierarchical heatmap in more detail, demonstrating the more pronounced level of downregulation in the chronic compared to the acute phase. Our results agree with the findings of Spann et al. [22], who reported the significant downregulation of the cholesterol biosynthesis pathway and the downregulated expression of genes involved in the production of cholesterol (*Hmgcs1*, *Hmgcr*, *Cyp51*, *Idi1*, and *Fdft1*). We also observed permanent mitochondrial dysfunction, suggested by the downregulation of functions/pathways related to mitochondria and ATP synthesis [23] (Fig. S18). The totality of the described events acts to the detriment of correct nervous system function and any regenerative attempts, as indicated by the large number of downregulated functions related to synapse regulation, neurotransmitter regulation, or nervous system development in all groups (Fig. S19–21).

Next, we estimated TF activity levels based on the expression levels of their target genes, using a methodology that considers whether TF-target interactions activate or repress said target gene (Table S11). Thus, the upregulation (respectively downregulation) of target genes of an activating (respectively inhibiting) TF becomes interpreted as TF activation following injury [normalized enrichment score (NES) > 0]. Conversely, activating (respectively inhibiting) TFs with downregulated (respectively upregulated) target genes are interpreted as lost TF function or deactivation following injury (NES < 0). We observed a higher prevalence of activated vs. deactivated TFs in all scenarios (Fig. S22A). This finding underscores the more substantial impact on TF activation during the early stages after SCI, which gradually decreases in the chronic phases. Figure 2B (left panel) depicts consistently dysregulated TFs shared between moderate and severe injury. TFs such as *Nfkb1*, *Stat1*, and *Stat3* become activated during injury progression, contributing to processes such as inflammatory response modulation [24–26]. This activation is consistent with the persistent upregulation of immune system-related pathways in the GSA, highlighting their role in sustaining the inflammatory response post-injury. Interestingly, *Srebf1* exhibits an ever-increasing gene expression pattern (Fig. 2C); however, this TF becomes differentially deactivated in all comparisons except M1. Both *Srebf1* and *Srebf2* (also deactivated) represent activators of lipid metabolism genes [27], which could explain the

previously described downregulation of fatty acid and cholesterol synthesis.

We used the gene consensus signatures matrix (Table S16) from moderate and severe injury separately as inputs to identify genes with similar expression patterns. We identified 19 (moderate injury) and 18 (severe injury) clusters of co-expressed genes and constructed a PPI network for each cluster. The extensive constructed networks displayed elevated levels of interconnection, indicating the functional association of genes with similar expression patterns. To gain deeper insights, we generated 261 subnetworks, conducted a functional enrichment analysis for each subnetwork, and then classified them into manually predefined biological categories of interest. Among the 261 generated subnetworks, we successfully classified 153 (Fig. S23). The remaining 108 subnetworks comprised only a few proteins without enriched functions. As observed in the GSA results, we found the prominent representation of categories such as nervous system, immune system, and metabolism; moreover, we observed notable functional similarity across severity levels. Figure 2D depicts cluster 11, subnetwork 1 for moderate injury, comprising genes related to the cell cycle (proteins in green, red, and purple also form a physical part of the same complexes). These genes possess an expression pattern characterized by an initial upregulation that decreases over time (Fig. 2E); as discussed previously, this explains the presence of enriched functions related to the cell cycle in T1 that decrease in subsequent phases. See Fig. S24 for a summary diagram of severity- and phase-specific biomarker genes and their associated pathological processes in SCI.

Consistency in temporal gene expression patterns between the mouse and rat

To validate and compare gene expression patterns obtained in our meta-analysis, we selected a mouse RNA-seq dataset from Li et al. [28], which possessed an experimental design similar to the studies included in our work. They induced injuries at the T9 level and collected samples from a spinal cord segment on different days post-injury (dpi), covering the four phases established in our work. We then followed the same pipeline applied to individual studies to generate gene expression patterns, ensuring their comparability with those generated in our meta-analysis. Tables S12–16 reports the DGE analysis results of each comparison and the gene expression patterns matrix.

We conducted a correlation analysis to compare gene expression patterns between the mouse and rat models (rat moderate injury vs. mouse; rat severe injury vs. mouse; rat moderate injury vs. rat severe injury), demonstrating a generally positive relationship. The density plot of correlation values indicates a median close to

0.5 in the three comparisons (Fig. 3A and Table S17). A total of 892 genes displayed a strong positive relationship ($r > 0.9$) between mouse and moderate rat injury, another 892 genes demonstrated a positive relationship between

mouse and severe rat injury, and 922 genes presented a positive relationship between moderate rat injury and severe rat injury. Among these, 198 genes positively correlated across all three comparisons (Fig. 6A). We next

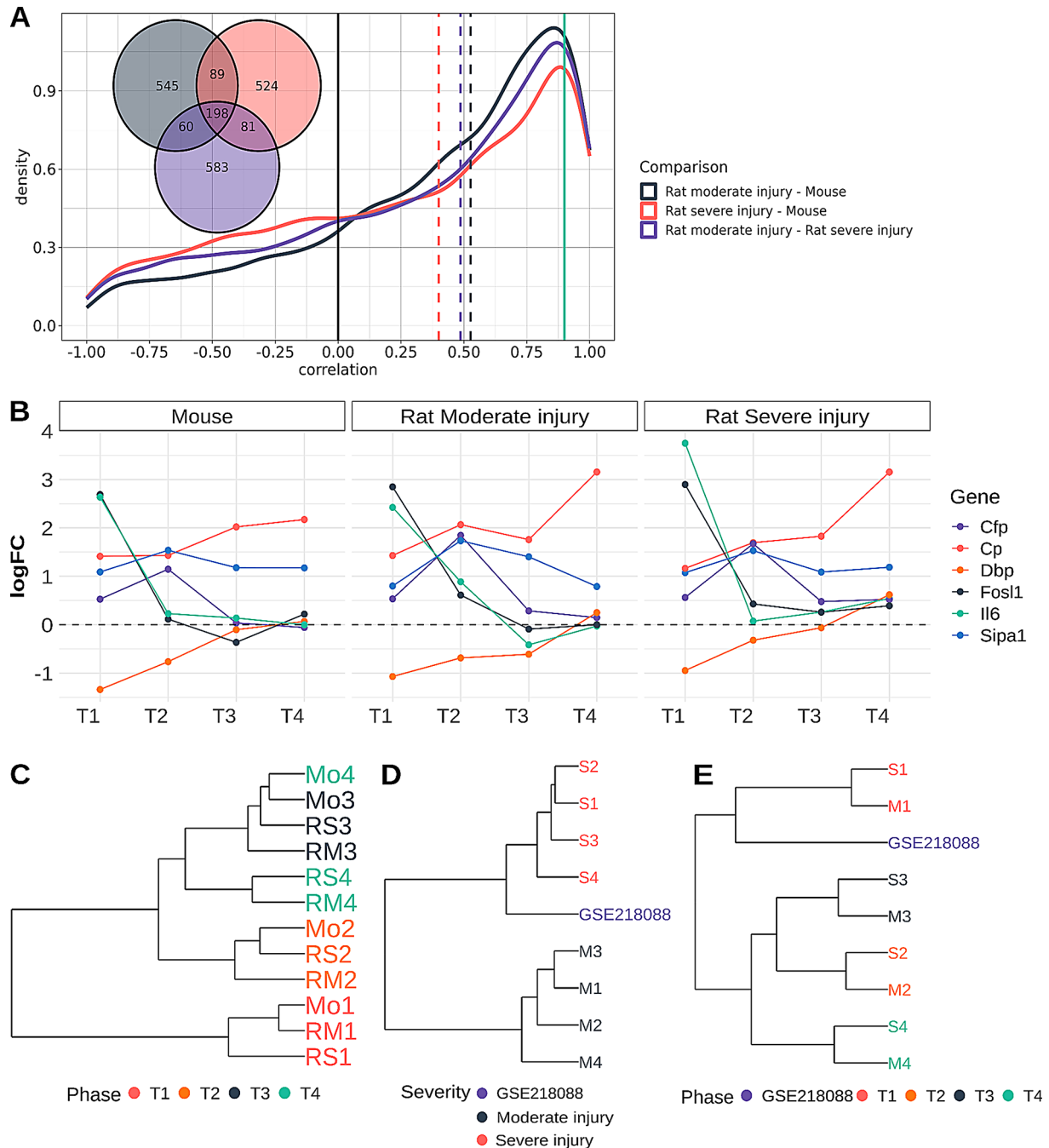


Fig. 3 Gene expression patterns comparison between rat meta-analysis and mouse dataset, and clustering analysis using biomarker genes in mouse and GSE218088 datasets. **(A)** Density plot of correlation values between gene expression patterns. Black denotes rat moderate injury vs. mouse; red denotes rat severe injury vs. mouse; and purple denotes rat moderate injury vs. rat severe injury. The green line represents a correlation coefficient of 0.9. Dashed lines represent the median correlation values for each comparison. The Venn diagram depicts the intersection of genes with a correlation coefficient greater than 0.9 in each comparison. **(B)** Comparison of expression patterns of phase-specific genes in mice and moderate/severe injury in rats. **(C)** Hierarchical clustering using phase-specific genes (*Fos1*, *Il6*, *Cfp*, *Sip1a1*, *Cp*, and *Dbp*) with meta-analysis signatures and the mouse dataset. **(D)** Hierarchical clustering using severity-specific genes with meta-analysis signatures and the GSE218088 transcriptional signature. **(E)** Hierarchical using phase-specific genes with meta-analysis signatures and GSE218088 transcriptional signatures

performed a clustering analysis using a curated set of potential phase-specific genes (*Fosl1*, *Il6*, *Cfp*, *Sipa1*, *Cp*, and *Dbp*) that displayed similar gene expression patterns across the three comparisons (Fig. 3B). Hierarchical clustering in Fig. 3C revealed a clear separation of groups based on time post-injury, similar to that observed in Fig. 1G.

In this case, the mouse T3 and T4 signatures become grouped within the same branch as M3 and S3 in the rat, which could be explained by slight differences in timings. Mouse T3 is defined as 28 dpi, and T4 is 42 dpi, whereas rat T3 covers 15–35 dpi, and T4 extends from 56 to 168 dpi. Longer intervals between phases could lead to more distinct differences in expression profiles, as the injury has additional time to stabilize.

Our comparative analysis with an SCI mouse model validated the gene expression patterns established in our meta-analysis and demonstrated a positive correlation between mouse and rat injury responses, supporting the reliability of the identified biomarker genes.

Proposed severity- and phase-specific biomarker genes effectively classify novel rat transcriptomic profiles

We used the GSE218088 dataset [29] published after the study search and selection period as a validation set, given that it meets the inclusion criteria established in the meta-analysis. We aimed to evaluate whether selected phase- and severity-specific biomarker genes could correctly classify a new transcriptomic profile. In this study, the authors indicated that the free fall of a 10 g hammer with a diameter of 2.5 mm produced the injury,

which is considered severe [30, 31]. The authors reported that they extracted spinal cord tissue three days after SCI, corresponding to the acute phase (T1) defined in our work.

Using the top 10 severity-specific genes (Table 1), we observed the clustering of the transcriptional signature of the GSE218088 dataset with the severe injury groups in our analysis (Fig. 3D). Additionally, using phase-specific biomarkers for T1, T2, and T4 (Table 1), we also observed the clustering of the transcriptional profile of GSE218088 with the T1 signatures from our meta-analysis (Fig. 3E). Therefore, this comparison demonstrates the robustness of the obtained results and the capacity of the biomarker genes to classify a new transcriptional profile.

Concordance between meta-analysis gene expression patterns and qPCR analysis

We aimed to validate the expression patterns our meta-analysis identified through experimental validation. Following severe injury induction, we extracted RNA from the injured spinal cord tissue in rats at T1, T2, T3, and T4 post-injury. We selected eight genes to validate expression profiles by qPCR - four TFs (*Cebpd*, *Hes1*, *Jun*, and *Onecut1*) given their functional relevance and four target genes of the TFs (*Il6*, *Vcam1*, *Vegfa*, and *Vim*) that also represent potential phase-specific biomarker genes (Fig. 4).

Il6 exhibited general overexpression with notably higher expression in T1 than in other phases, where gene expression remained similar to pre-injury levels. *Vcam1* became downregulated in T1 followed by a

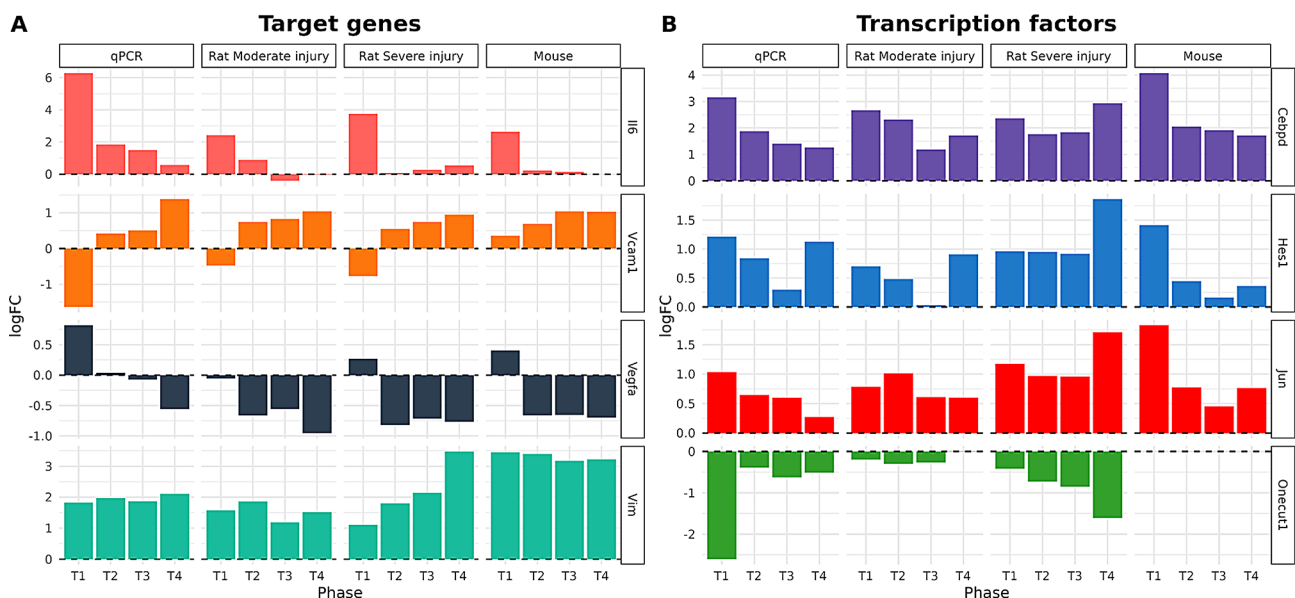


Fig. 4 Comparison of gene expression patterns for selected transcription factors and their targets for experimental validation. qPCR values obtained by calculating the logFC of the expression at each time vs. the expression of the uninjured samples in qPCR. Rat Moderate injury indicates the expression pattern obtained in the meta-analysis for moderate injuries. Rat Severe injury indicates the expression pattern obtained in the meta-analysis for severe injuries. Mouse indicates the expression pattern obtained in the mice dataset

gradual upregulation in expression over time, except in the mouse dataset, where we only appreciated a gradual increase in expression. Oppositely, *Vegfa* became upregulated in T1 and downregulated in the other phases. *Vim* expression analysis confirmed the constant upregulation, although qPCR did not validate a potential role for *Vim* as an S4-specific biomarker.

Cebpd, *Hes1*, and *Jun* displayed similar upregulated gene expression patterns in the qPCR analysis, meta-analysis, and mouse dataset, although lower consistency existed in the expression patterns across all four systems. Contrarily, *Onecut1* presented a different pattern of change, although we confirmed constant downregulation of gene expression over time.

In addition, we conducted a correlation analysis to compare the logFC values obtained from qPCR with those derived from the meta-analysis and mouse dataset (Fig. S25). For target genes, 10 of 12 qPCR comparisons had strong Pearson correlations above 0.85; in contrast, only 5 of 11 comparisons for TFs exceeded 0.7.

Taken together, although reproducing the exact gene expression patterns remained challenging, this validation step confirmed general dysregulation patterns or at least the direction of dysregulation at specific phases after injury.

Severity-specific rat biomarker genes predict injury prognosis from human SCI patient blood samples

To investigate the potential clinical translation of the severity-specific biomarker genes identified in rats to the prediction of injury prognosis from blood samples of human SCI patients, we analyzed the GSE151371 dataset [32] containing gene expression profiles of human blood samples collected in the first 10 days after SCI. Human SCIs are categorized based on severity and prognosis using the American Spinal Cord Injury Association (ASIA) with a 5-grade scale - the American Impairment Scale (AIS) - ranging from A-E (moving from more to less severe). Grade A denotes complete sensory and motor loss; Grade B signifies complete motor loss but preserved sensation; Grade C and D represent various degrees of motor function preservation, while Grade E indicates normal sensory and motor function [33].

To achieve a similar scenario to our rat-based meta-analysis, we selected samples from AIS A and AIS D to ensure similarity in severity between the two biological systems. After DGE analysis between groups, we identified 931 genes (FDR < 0.1; Table S18). Next we compared this list with the 282 severity-specific genes previously identified in rats (Fig. 5A). We found twelve intersecting genes (*EXT1*, *FBN1*, *FOSB*, *GNAO1*, *GRB10*, *MMP9*, *NFE2*, *PRF1*, *SLC25A23*, *SNAI1*, *ST6GALNAC3*, and *STX11*) (Fig. 5B), whose expression patterns in the

GSE151371 dataset were characterized by increasing dysregulation as SCI severity increases (Fig. S26).

We then used this 12-gene signature to analyze the ability to stratify groups according to severity by clustering analysis in rats and humans. Human blood sample analysis revealed the presence of three clusters: severe injury, moderate injury, and healthy controls (Fig. 5C), while the gene consensus signatures demonstrated stratification based on the severity level in rats (Fig. 5D). These findings indicate that expression levels of the 12 potential biomarker genes can delineate severity-specific subgroups in human blood and rat spinal cord samples.

Meta-SCI app - an interactive and user-friendly platform to explore results

We developed the Meta-SCI app (<https://metasci-cbl.shinyapps.io/metaSCI/>), an interactive web application that provides a user-friendly interface to consult and visualize the results obtained in this work, allowing users to gain a deeper understanding of the underlying mechanisms of SCI. This application consists of eight main modules (Fig. 6), allowing users not only to explore all the generated results but also perform further analysis and research with the available tools. For further information on the modules of the Meta-SCI app, consult the “Help” section.

Discussion

SCI represents a complex challenge that demands novel approaches to better understand the underlying disease-associated mechanisms. Here, we present a transcriptomic meta-analysis consolidating the most significant number of studies/samples regarding rat SCI datasets to our knowledge. Furthermore, we integrate diverse experimental models based on severity and phase post-injury. As a pioneering effort, we also establish a freely accessible transcriptomic reference for SCI research.

The strength of our work emerges from the generation of transcriptomic consensus signatures within established groups. Applying uniform processing and integration through meta-analysis enhances statistical robustness when determining the magnitude of gene alterations, mitigating inherent dataset heterogeneity and biases stemming from disparate pipelines – a significant feat, given that studies with identical experimental designs can yield contradictory expression changes for the same gene [34]. Experimental validation represents another strength of our research, which we demonstrated via (i) qPCR of eight gene signatures, confirming the direction of dysregulation in all cases; (ii) bioinformatic analysis, finding a positive correlation in temporal transcriptional changes between rat and mouse; and (iii) the correct classification of an external transcriptional signature using proposed severity- and phase-specific biomarker genes.

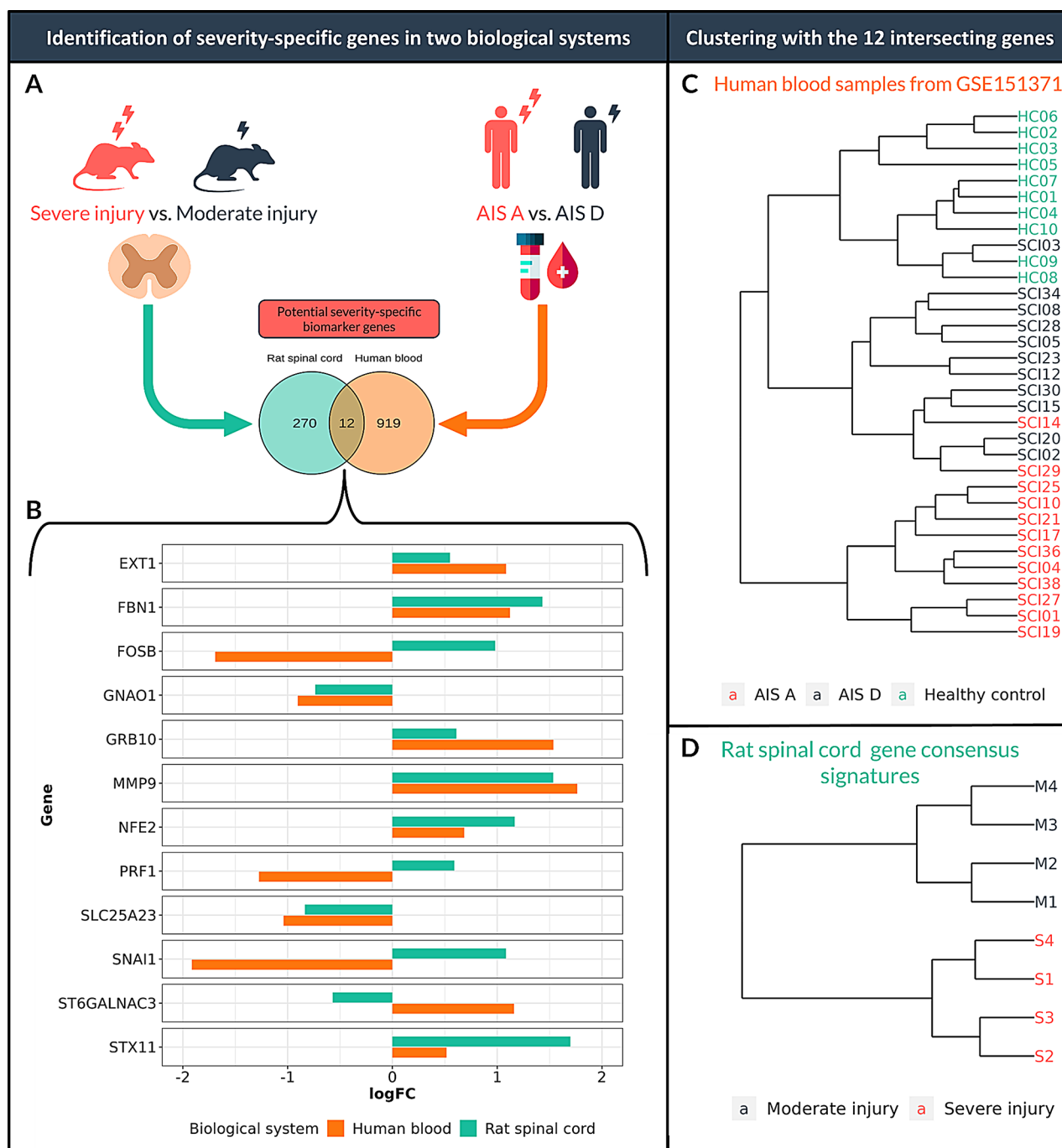


Fig. 5 Severity-specific biomarker genes stratify samples in human and rat SCI models. **(A)** Schematic illustration of the approach to identify severity-specific biomarker genes common to the two biological systems under study. **(B)** Barplot comparing the logFC of the 12 intersecting genes. Orange bars indicate the logFC values after comparing AIS A vs. AIS D in human samples. Green bars indicate logFC after comparing the consensus logFC in severe injuries and consensus logFC in moderate injuries obtained in rat meta-analysis. **(C)** Hierarchical clustering uses the 12-gene signature in human blood samples from the GSE151371 dataset. **(D)** Hierarchical clustering using the 12-gene signature in rat spinal cord gene consensus signatures obtained in the meta-analysis

Our work facilitates the comparison of gene expression levels, pathways, and TF activity across time/injury severities. Furthermore, direct identification of gene expression levels associated with specific pathways or TF targets is possible. While one of our study’s strengths

lies in assembling 14 studies and 273 samples, unequal representation across experimental groups represents a limitation, highlighting an emphasis on acute and a lack of samples in chronic phases. As far as our knowledge extends, Squier et al. [35] previously integrated the larger

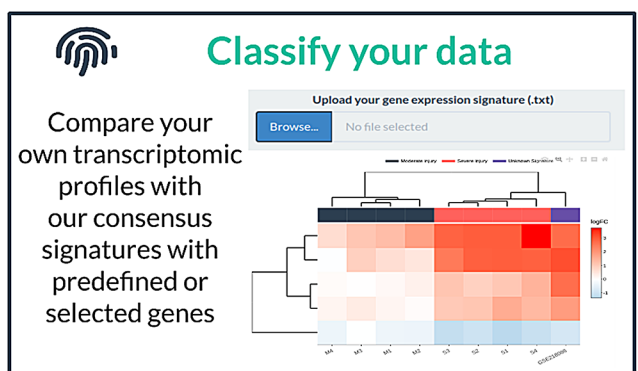
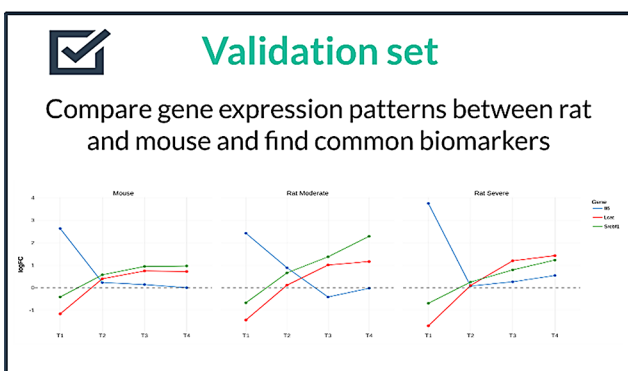
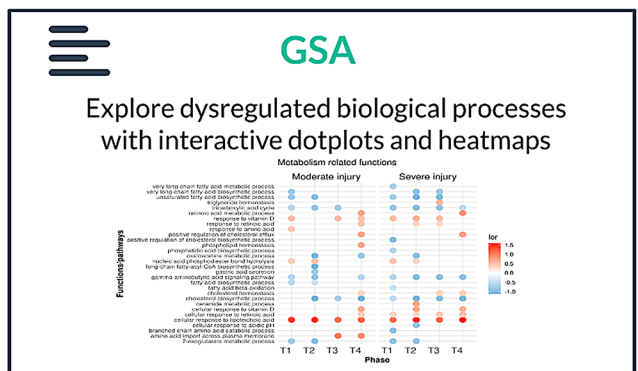
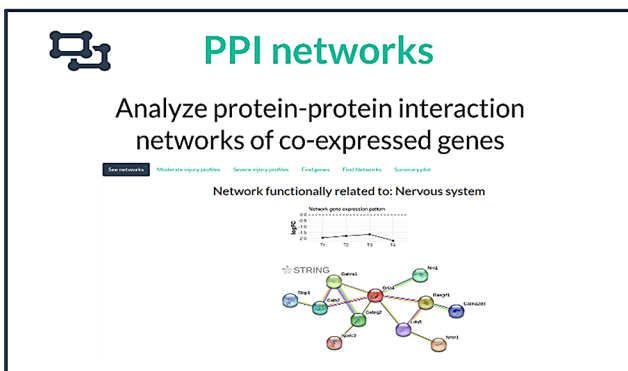
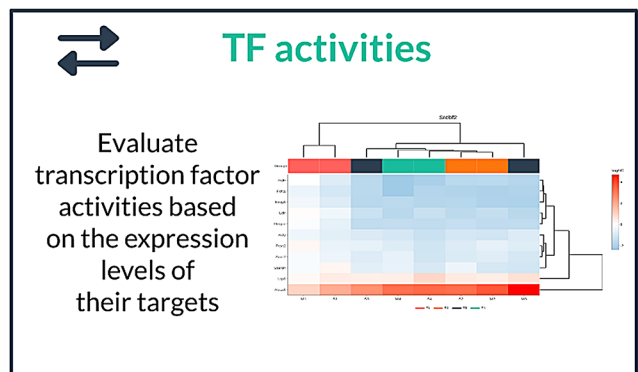
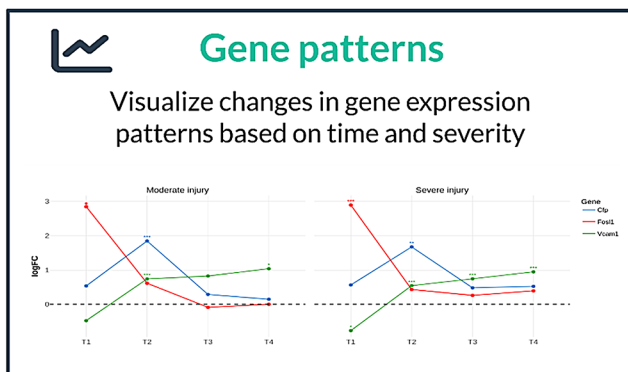
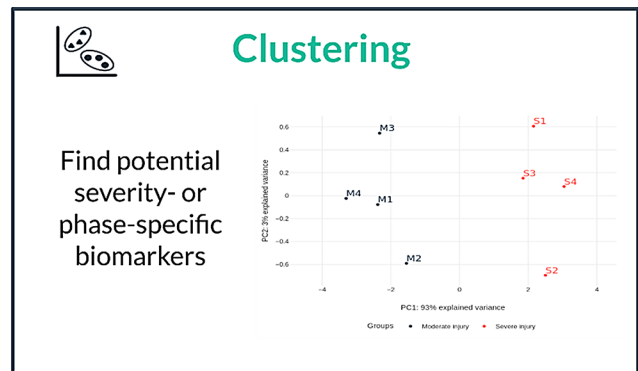
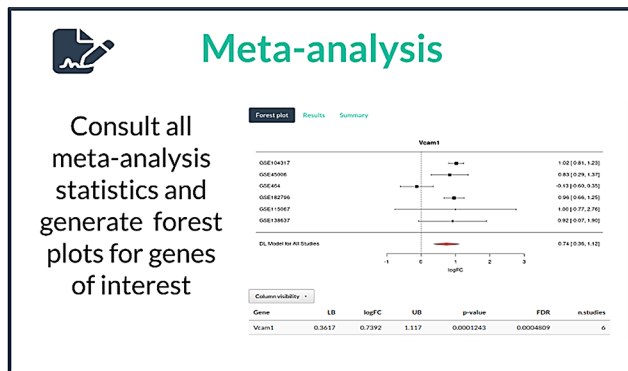


Fig. 6 Overview of the main Meta-SCI app modules

number of rat SCI transcriptomic datasets. Nevertheless, our research represents a progress, as we incorporated a more comprehensive array of diverse datasets (14 vs. 3) and employed more sophisticated integration methods using meta-analysis instead of an intersection of results. This underscores the necessity to publish data following FAIR principles (findability, accessibility, interoperability, and reusability) [36], as certain studies do not provide data or adequate sample descriptions. Another potential limitation arises from including datasets derived from diverse technologies and platforms (10 microarrays and 4 RNA-seq experiments). However, the standardized reanalysis and subsequent integration after DGE analysis effectively captured changes in transcriptional regulation [9].

This study generated eight consensus transcriptional profiles that comprehensively characterized each pre-defined group. These transcriptional profiles serve a dual purpose: first, they provide insight into phase- and severity-specific expression patterns of genes, and second, they are used for the identification of potential biomarkers and functional characterization. Various sources reinforce the robustness of these expression profiles. Previously, Tica et al. [37] combined four transcriptomic and proteomic datasets to identify genes/proteins persistently dysregulated at 7 days and 8 weeks post-injury. They found 40 upregulated and 48 downregulated genes/proteins, consistently matching our meta-analysis results. Notably, our research identified one of these genes - *Vim* - as consistently upregulated across all time points after SCI, corroborating results from the meta-analysis, the mouse dataset, and qPCR validation. We also validated the expression profiles of the meta-analysis by comparing them with the expression profiles of a mouse dataset [28] that shared a very similar experimental design to those studies included in our work. We observed an overall positive correlation between mouse and rat gene expression patterns for moderate and severe injury. While the exact replication of expression patterns posed challenges, qPCR-based validation reaffirmed the direction of dysregulation (upregulation/downregulation) at specific time points. Overall, these transcriptomic consensus signatures provide insight into how gene expression patterns evolve, offering valuable information regarding the development of potential therapeutic strategies suitable for each SCI phase.

We identified biomarker genes distinguishing moderate and severe injuries, displaying significant and persistent dysregulation in severe injuries. The downregulated genes play roles in the functions and development of the nervous system and synapses. These findings mirror the increased loss of function associated with severe injury due to more extensive damaged tissue and complete axonal rupture. The upregulated genes are associated with

tissue remodeling and extracellular matrix organization. Notably, 45 of these genes are translated into proteins that locate to the extracellular region. In severe injuries, these genes might become activated to regulate mechanisms involved in wound healing and fibrosis [38]. By employing the top 10 severity-specific genes, we effectively classified an external dataset involving a severe rat injury, demonstrating their validity. The expression profiles of the identified severity-specific genes make them suitable as prognostic biomarkers. Since no significant expression changes occurred in moderate damage, but considerable and persistent dysregulation occurred in severe injuries, these genes can be employed at the early stages of injury to predict progression. Among potential severity biomarkers, we identified the *Mmp9* and *Mmp23* matrix metalloproteinases (MMPs), which exhibited significantly higher upregulation in severe compared to moderate injury. Previous studies suggested MMPs as potential predictive biomarkers for worse neurological outcomes in human patients as well as in rat and canine models [38–42]. This consistency across species underlines the reliability and potential application in clinical research as prognosis biomarkers. In addition, Microtubule-Associated Protein 2 (*Map2*) has previously been proposed as a severity biomarker [40, 43]. Our results indicate a greater downregulation of *Map2* (and *Map7*) expression in severe injury, which could represent a new candidate biomarker gene for future studies.

We also identified biomarker genes that allowed for phase-specific stratification of transcriptomic profiles regardless of severity. The acute phase (T1) - the most characteristic and readily distinguishable phase - provided the highest number of potential biomarker genes. This may be explained by the cascade of events triggered by the initial trauma, including the activation of stress and inflammatory response mechanisms to contain the injury [1, 17]. Additionally, we also observed a great activation of genes related to the cell cycle, driven by the proliferation/activation of mitotic cells (such as microglia and astrocytes), as well as the initiation of apoptotic processes in damaged cells [18, 19]. In fact, it has been reported that inhibition of cell cycle gene expression may improve motor and cognitive recovery [44–47]. Subacute phase-specific genes, including complement-related genes (e.g., *Cfp*, *C1qa*, *C1qb*, and *C1qc*), exhibited a distinct gene expression pattern peaking at T2. This pattern aligns with the dynamic behavior of cells such as macrophages and microglia that express and secrete complement proteins [15, 16]. Monocytes migrate to injury sites and differentiate into macrophages at approximately 3 dpi, culminating in a peak response at around 7 dpi, while resident microglia reach an activation peak one-week post-injury [48, 49]. Utilizing a combination of phase-specific genes supports the accurate classification

of transcriptomic profiles for meta-analysis data and new transcriptomic profiles, such as those in the GSE218088 dataset. Additionally, while certain genes display species-specificity, common genes (such as *Fosl1*, *Il6*, *Cfp*, *Sipa1*, *Cp*, and *Dbp*) can be used for the temporal classification of rat and mouse samples. Experimental validation of *Il6*, *Vcam1*, and *Vegfa* confirmed the expression patterns observed in the meta-analysis and validated their similarity in the mouse dataset. Thus, our study identified phase-specific biomarkers that may aid in selecting therapies based on transcriptomic profiles and improve patient stratification.

Our work provides a functional framework for assessing the degree of dysregulation in biological functions of interest. Our findings align with previous SCI research, characterized by the maintained upregulation of functions related to the immune system and the downregulation of processes associated with the nervous system function and development. This phenomenon is influenced by other processes that sustain an unfavorable environment for functional recoveries, such as disturbed ionic homeostasis, vascular injury, ischemia, free radical stress, cell death [13, 17, 50], mitochondrial dysfunction [23], metabolic alterations (including the downregulation of lipid and cholesterol metabolism) [22], or extracellular matrix remodeling [51]. Considering this complex context, any strategy for developing effective therapies should include a combination of multiple targets, considering the interconnected nature of these systems. At the functional level, we observed differences between phases, with the decreasing significance of pathways related to cell cycle and RNA transcription as time progresses post-injury particularly noteworthy. However, in contrast to gene-level results, we did not identify substantial differences between severities. Likewise, the constructed co-expression networks, comprising different genes with altered expression based on severity, demonstrated similarities in the enriched functions' quantity and nature. This analysis corroborates the functional interconnection of genes with similar expression patterns [52, 53] and agrees with the study of De Biase et al. [54], which failed to report consistent alterations in functional patterns associated with injury severity, even given the apparent variations occurring at the gene expression level. This phenomenon may be explained by the design of functional enrichment techniques that capture the coordinated action of gene groups. Consequently, even though specific genes may display more pronounced dysregulation in severe injuries, their collective direction points toward the same outcome.

Our study also provides a way to infer the activity of master transcriptional regulators represented by pioneering evaluation of TF activity based on the expression levels of target genes, providing a new perspective

for more efficient therapeutic interventions. In addition, we experimentally validated four TFs. *Hes1* - a transcriptional repressor involved in neurogenesis [55] - displayed overexpression in our meta-analysis and the experimental validation and differential activation in all experimental groups. Previous studies support these findings, demonstrating *Hes1* overexpression after SCI [56] and emphasizing the role of *Hes1* in promoting neurogenesis through inhibition of its target genes, consequently enhancing functional recovery [57]. *Onecut1* - a transcriptional activator regulating the production, diversification, distribution, and maintenance of various neuronal populations [58–60] - became downregulated following SCI; while we experimentally validated this result, the results were not wholly consistent with the expression pattern obtained from the meta-analysis, possibly thanks to inter-experimental data heterogeneity. Activity inference analysis indicated *Onecut1* deactivation, especially in the early phases of injury. These findings suggest that *Onecut1* overexpression or increased *Onecut1* activity could benefit neuronal development and function. Our bioinformatic and experimental results also indicated upregulation of *Cebpd* - a transcriptional activator that regulates genes involved in immune responses [61] - after injury, accompanied by differential activation in acute phases. Previous studies reported *Cebpd* overexpression following injury [61, 62] and enhanced expression during functional recovery in mice deficient in this gene [62]. *Jun* - a transcriptional activator highly induced following neuronal damage [63, 64] - became consistently overexpressed and activated in all experimental groups; in a related study, Zhang et al. proposed that miR-152 overexpression inhibited inflammatory responses and promoted functional recovery by inhibiting *Jun* [64].

We believe the identification of a 12-gene signature predicting injury severity in human blood and rat spinal cord data is of great interest. The major challenge involves the inability to obtain expression data from human spinal cord samples and the absence of datasets comparing moderate and severe injuries in rat blood samples, which prevents direct tissue comparisons. For these reasons, identifying common biomarkers between tissue and blood across species is valuable. It suggests that certain biological processes may be conserved and detectable in peripheral blood, even if the injury is localized to the spinal cord. Among these 12 genes, *MMP9* has already been proposed as a predictive biomarker across various species [39, 41, 65]. Also, while identifying a biomarker in blood and tissue can be challenging, there exist documented cases where this has been successful. For example, Qi et al. identified a gene signature, including *MMP9*, that could differentiate glioblastoma patients based on transcriptomic profiles derived from both blood and tumor tissue [66]. This suggests that

other genes proposed in our study may also hold prognostic value in both species. The clinical application of this signature could be valuable, enabling patient stratification through simple and non-invasive techniques such as blood extraction and transcriptional analysis, making it easier to implement in clinical settings, such as hospitals. Although the ASIA system, accompanied by the anatomical evidence of the extent of the affected and preserved tissue by magnetic resonance imaging, represents the standard for predicting SCI severity, a need exists to find new operative and non-invasive methods for prognosis. The ASIA system relies on neurological status evaluations through sensory and motor exams; however, this method suffers from limitations [32]. Further investigation will be required to explore the prognostic capacity of these genes in detail with larger sample sizes in humans and additional relevant models.

The development of the Meta-SCI app during this study offers an additional dimension. This platform extends beyond a mere results repository; Meta-SCI serves as an analysis tool for the research community. Also, Meta-SCI includes two injury models, allowing researchers to choose which best suits their needs. Consequently, the Meta-SCI app emerges as a valuable resource for hypothesis generation and validation and constitutes a transcriptional reference database for studying SCI.

Our study offers a comprehensive systems biology frame of SCI, providing a holistic view at the gene and functional levels involving the dimensions of severity and phase. We identified potential biomarker genes that effectively stratified transcriptomic profiles based on phase and severity, offering critical insights into SCI progression. Thanks to our user-friendly Meta-SCI web application, researchers can explore this extensive results repository, tailoring their investigations to their fields of interest. Our study sheds light on the intricate mechanisms underlying SCI and equips researchers with the means to translate these insights into diagnostic and therapeutic interventions.

Methods

Study search and selection

A systematic review and selection of studies was conducted in September 2022. The search was performed in two public databases for transcriptomic data - GEO [10] and ArrayExpress [11] - according to PRISMA [12] statement guidelines and carried out using the keywords “spinal cord injury.” The inclusion criteria were: (1) organism, *Rattus norvegicus*; (2) tissue, thoracic spinal cord; and (3) RNA sequencing or microarray data from Affymetrix or Agilent used as gene expression platforms. The exclusion criteria were: (1) studies without control samples (sham or naive rats); (2) individual samples from rats that had

received any type of treatment; and (3) samples rostral or caudal to the epicenter of the injury.

Injury severity was classified into moderate and severe injury. The severe group included lesions resulting from a spinal cord impact of ≥ 200 kdyn, a 10 g weight drop from 50 mm, or a complete transection of the spinal cord; meanwhile, injuries not meeting these criteria were considered moderate (Table S2). Additionally, four phases of injury were defined based on the timeline post-injury and when samples were collected: acute (0–3 days, T1), sub-acute (4–14 days, T2), early chronic (15–35 days, T3), and late chronic (over 35 days, T4). Control groups included samples from rats, either sham-operated or non-operated naive rats. For a comprehensive view of the experimental design, consult Figure S27 for the SCI modeling diagram, Table S2 for the specific injury method used, and Table S3 for detailed annotations for each sample.

Data preprocessing

For microarray studies, normalized data were downloaded with the GEOquery package and probes were annotated to their corresponding gene symbol using platform-specific annotation packages. For RNA-seq studies, raw count matrices were manually downloaded from GEO, and identifiers were converted to gene symbols using the org.Rn.eg.db package. In all cases, the median of the expression values of duplicated identifiers was calculated.

Exploratory analysis

An exploratory analysis was performed (including boxplot, PCA, and clustering analysis) to observe sample distribution in the groups of interest and evaluate anomalous behavior and possible batch effects. Samples from the GSE183591 study were taken in two different series, separated into two blocks in the PCA. This batch effect was taken into consideration for DGE analysis. The negative values detected in boxplots for the GSE2599 and GSE464 datasets were normalized by adding the minimum of all values followed by a logarithmic transformation of the data.

Differential gene expression analysis

Each injury group was compared with its corresponding control within the study to identify DEGs. DGE analysis of microarray platforms used the limma package [67]. To ensure comparable results between technologies, RNA-seq datasets were analyzed using the limma-voom pipeline, which involves the removal of genes with low counts and a logarithmic transformation of the expression matrix. P-values were corrected with the Benjamini–Hochberg (BH) method [68].

Gene expression meta-analysis

DGE results were integrated to obtain a transcriptional consensus signature for each comparison. A meta-analysis was performed for each gene in at least two studies in each comparison. The random-effects model proposed by Der Simonian & Laird [69], implemented in the metafor package [70], was used to evaluate the combined effect. This method weighs the heterogeneity of each study and incorporates their inherent variability into the overall estimate of the measure of effect. Consequently, studies with greater variability will have lower weight in this measure. In this case, logFC values were used to measure the effect, while the variance was used to measure variability. Thus, values for the p-value, logFC, and 95% confidence interval (CI) were calculated for each gene evaluated in the meta-analysis. Since multiple meta-analyses were performed, p-values were adjusted using the BH method. Adjusted p-values lower than 0.1 were considered significant. Funnel and forest plots were used to assess the variability and measure each study's contribution to the meta-analysis.

Clustering analysis

All clustering analyses were performed on the gene consensus signature matrix. This matrix was constructed with consensus logFC values from the meta-analysis, selecting genes evaluated in all groups and significant in at least one group. The mixOmics package was used for PCAs [71]. For hierarchical clustering analysis, the Euclidean distance was first calculated as input for the hclust function.

Biomarker gene identification

In this context biomarker genes were defined as those displaying more significant deregulation in certain groups of interest than others, allowing the stratification of different groups based on their expression pattern. A limma test was applied to identify possible biomarker genes that could classify samples according to severity/phase. The four severe groups were compared against the four moderate groups of samples to elucidate severity-specific biomarker genes. Phase-specific biomarker genes common to both severities and specific to moderate or severe injury were also explored. Detailed comparisons are listed in Table S4. Subsequently, the top 10 genes with the lowest p-values from each comparison were selected to assess their classification ability via clustering analysis comprising PCA and hierarchical clustering.

Gene set analysis

Functional enrichment analysis was performed for each gene consensus signature with the GSA method implemented in the mdgsa R package [72]. A gene ranking and functional annotation are required as input for GSA. The

ranking is made by ordering all genes according to the p-value obtained in meta-analysis and the logFC value sign. For functional enrichment annotation, three annotation databases have been included: the biological processes of Gene Ontology [73], KEGG pathways [74], and Reactome pathways [75]. Gene sets with less than 10 or more than 500 genes were excluded. P-values were corrected with the BH method.

Transcription factors activities

The identification of differentially active TFs used the msviper function of the viper package [76] with each of the gene consensus signatures as input. Mouse regulons from the DoRothEA package [77] with a confidence level of A, B, C, or D were selected, excluding those with less than 10 genes (Table S11). The p-values were corrected using the BH method.

Construction of gene co-expression networks

First, genes with similar expression patterns were found using the clust software [78] with the following arguments: -n 0 -t 100 -cs 4. Gene consensus signature matrices from moderate and severe injury were used separately as input. A PPI was then constructed for each cluster of co-expressed genes obtained from clust software. The STRINGdb package with the interactions of STRING version 11.5 [79] and medium confidence of 0.400 were used to build PPI networks. The PPI network of each cluster was divided into different subnetworks of more closely related genes using the fastgreedy algorithm implemented in the get_clusters function.

Each subnetwork was then classified into manually pre-defined functional categories of interest. The get_enrichment function was first used to obtain overrepresented functional terms in each subnetwork. Subsequently, the biological processes were selected from the Gene Ontology, KEGG, and Reactome pathways, ad hoc classifying them into pre-established general categories. Finally, the frequency distribution of each category was calculated for each subnetwork, assigning the category with the highest frequency as that which best defines the network.

Bioinformatic validation datasets

For the mouse transcriptomic dataset, a normalized count matrix provided from the supplementary material provided by Li et al. [28] (<https://doi.org/10.6084/m9.figshare.17702045>) was downloaded. Samples representative of the four temporal phases established in our study (1, 7, 28, and 42 dpi) and controls were selected (Table S19). For the GSE218088 dataset, the normalized expression matrix was downloaded using GEOquery, and the probes were annotated to the gene symbol. Those genes that displayed significance in at least one comparison and were present in all groups of our meta-analysis were selected

for both datasets. A DGE analysis using the limma package was performed, comparing each injured group against uninjured controls.

Experimental validation via qPCR

A severe traumatic SCI model in adult female Sprague Dawley rats was employed for RNA isolation and qPCR in silico data validation. The animals were housed at the Animal Experimentation Unit of the Research Institute Príncipe Felipe (Valencia, Spain) under standard conditions. All experimental procedures adhered to the guidelines established by the European Communities Council Directive (86/609/ECC), the Spanish Royal Decree 53/2013, and the Animal Care and Use Committee of the Research Institute Príncipe Felipe (2021/ VSC/ PEA/0032).

Rats were subcutaneously pre-medicated with morphine (2.5 mg/kg) and anesthetized with 2% isoflurane in a continuous oxygen flow of 1 L/min. Laminectomy was performed on thoracic vertebrae 8–9 to expose the spinal cord, and severe SCI was induced at the thoracic vertebrae 8 level by contusion, applying a force of 250 kdyn using the Infinite Horizon Impactor, as previously described [80]. Post-surgery care included manual bladder drainage twice a day until vesical reflex recovery and subcutaneous administration of 5 mg/kg of Enrofloxacin (Alsir) for seven days, as well as 0.1 mg/kg of buprenorphine twice a day for four days after each intervention.

At each endpoint: 1 dpi ($n=3$), 7 dpi ($n=3$), 28 dpi ($n=4$), and 56 dpi ($n=4$) after injury to represent (T1, T2, T4, and T8, respectively), animals were overdosed of sodium pentobarbital (100 mg/kg) and transcardially perfused with a 0.9% saline solution. Spinal cord tissue was extracted, and the injury epicenter was immediately frozen in liquid nitrogen and stored at -80°C until use. RNA extraction was performed using the TriZol standard method, followed by an additional cleanup step using RNeasy MinElute Cleanup (Qiagen, Germany) to ensure sample quality ($A_{260}/A_{280} \approx 2$ and $A_{260}/A_{230} \geq 1.8$). Reverse transcription was performed using the high-capacity RNA-to-cDNA™ kit (Applied Biosystems, Massachusetts, USA).

Specific primers (Table S20) for each gene of interest were designed using primer-BLAST (NCBI, Maryland, USA) and validated by efficiency curve performance. qPCR was conducted in triplicate using AceQ SYBR qPCR Master Mix (ThermoFisher) in the Light-Cycler 480 detection System (Roche, Basel, Switzerland). Ct data were calculated using the LightCycler 480 relative quantification software (Roche, Basel, Switzerland). GAPDH mRNA levels served as an internal control for normalization.

Analysis of human blood samples

The GSE151371 normalized gene expression matrix was downloaded from GEO, and the expression values were log-transformed. The samples corresponding to the AIS A, AIS D, and the healthy control groups were then selected for further analysis (Table S21). DGE analysis was then performed to compare AIS A vs. AIS D with the limma package following the same pipeline as the previous analyses. Finally, significantly altered genes ($\text{FDR} < 0.1$) were selected to compare with the list of rat biomarker genes. The list of intersecting genes was used for the clustering analysis of both biological systems. The healthy controls from the GSE151371 dataset were also included for visualization and clustering analysis.

Meta-SCI app

Meta-SCI app is powered by the RStudio Shiny package and deployed on a shinyapps.io server, available at <https://metasci-cbl.shinyapps.io/metaSCI>. Plots are generated using ggplot, plotly, and heatmaply. All data processing and analysis are conducted using R.

Supplementary Information

The online version contains supplementary material available at <https://doi.org/10.1186/s12967-024-06009-6>.

Supplementary Material 1: Table S1. Studies included in meta-analysis. GEO series ID, platform, year and publications associated from selected datasets are indicated. Table S2. Injury method for each study. GEO series ID, injury method and category assigned for meta-analysis. Table S3. Sample annotation. GEO series ID, sample Id, group, severity level, phase and time for each sample. Table S4. Summary of sample distribution. Barplots showing the sample distribution by study, severity and phase. Table S5. Comparisons applied for specific biomarkers identification. Table S6. Severity-specific markers. Limma test results of comparison (S1, S2, S3, S4) vs. (M1, M2, M3, M4). Table S7. T1-specific biomarker genes. Limma test results of comparison (M1, S1) vs. (M2, M3, M4, S2, S3, S4). Table S8. T2-specific biomarker genes. Limma test results of comparison (M2, S2) vs. (M1, M3, M4, S1, S3, S4). Table S9. T3-specific biomarker genes. Limma test results of comparison (M3, S3) vs. (M1, M2, M4, S1, S2, S4). Table S10. T4-specific biomarker genes. Limma test results of comparison (M4, S4) vs. (M1, M2, M3, S1, S3, S4). Table S11. Interactions TF-target. Table S12. Li et al., 2022 DGE analysis results (1 dpi vs. control). Table S13. Li et al., 2022 DGE analysis results (7 dpi vs. control). Table S14. Li et al., 2022 DGE analysis results (28 dpi vs. control). Table S15. Li et al., 2022 DGE analysis results (42 dpi vs. control). Table S16. Mouse gene expression patterns matrix. Table S17. Correlation analysis. Table S18. GSE151371 DEG analysis results (AIS A vs. AIS D). Table S19. Li et al., 2022 mouse dataset sample information. Table S20. Primer sequences. Table S21. GSE151371 metadata.

Supplementary Material 2: Fig. S1. Prisma diagram. Fig. S2. Summary of sample distribution. Fig. S3. Overview of gene expression meta-analysis results. Fig. S4. Hierarchical heatmap of severity-specific biomarkers. Fig. S5. PPI network for down-regulated severity-markers. Fig. S6. PPI network for up-regulated severity-markers. Fig. S7. Group classification using top 10 T1-specific biomarkers. Fig. S8. Group classification using top 10 T2-specific biomarkers. Fig. S9. Group classification using top 10 T3-specific biomarkers. Fig. S10. Group classification using top 10 T4-specific biomarkers. Fig. S11. PPI network for up-regulated T1-specific markers. Fig. S12. PPI network for down-regulated T1-specific markers. Fig. S13. PPI network for down-regulated T2-specific markers. Fig. S14. PPI network T4-specific markers. Fig. S15. Gene set analysis reveals altered functions/pathways across time and severity after injury. Fig. S16. Dotplot of selection of down-regulated metabolism functions. Fig. S17. Hierarchical heatmap of genes in GO term

GO:0006695 (cholesterol biosynthetic process). Fig. S18. Dotplot of mitochondria related functions. Fig. S19. Dotplot of neurotransmission related functions. Fig. S20. Dotplot of synopsis related functions. Fig. S21. Dotplot of nervous system development related functions. Fig. S22. Summary of transcription factor activity inference analysis. Fig. S23. Summary of co-expression network results. Fig. S24. Diagram illustrating severity- and phase-specific biomarker genes associated with pathological processes in SCI. Fig. S25. Pearson correlation coefficient after comparing logFC values obtained in qPCR analysis with those from the rat meta-analysis and mouse dataset. Fig. S26. Normalized expression of 12 gene severity-markers in GSE151371 dataset. Fig. S27. Diagram showing the different SCI injury models and experimental design.

Acknowledgements

The authors thank the Principe Felipe Research Center (CIPF) for providing access to the cluster, co-funded by European Regional Development Funds (FEDER) in the Valencian Community 2014–2020. The authors also thank Stuart P. Atkinson for reviewing the manuscript.

Author contributions

Conceptualization: FGG. Methodology: RGR, MRH, BMR, VMM, FGG. Investigation: FGG, MRH, BMR, VMM, RGR. Visualization: RGR, MRH. Supervision: MRH, VMM, FGG. Writing - original draft: RGR, MRH, BMR, VMM, FGG. Writing - review & editing: RGR, MRH, BMR, VMM, FGG.

Funding

This research was supported and partially funded by the Institute of Health Carlos III (project IMPaCT-Data, IMP/00019), co-funded by ERDF, “A way to make Europe”; PID2021-1244300A-I00 funded by MICIU/AEI/10.13039/501100011033 and by FEDER, UE; and CIAICO/2023/149 funded by the Conselleria de Educaci3n, Cultura, Universidades y Empleo de la Generalitat Valenciana.

Data availability

All data needed to evaluate the conclusions in the paper are present in the paper and/or the Supplementary Material. All data and results generated in this study are freely available through the Meta-SCI app: <https://metasci-cbl.shinyapps.io/metaSCI>. Transcriptomic data are available at GEO under accession numbers: GSE183591, GSE182796, GSE138637, GSE133093, GSE115067, GSE102964, GSE104317, GSE93249, GSE52763, GSE45006, GSE46988, GSE29488, GSE2599, GSE464, GSE151371 and GSE218088. The code developed for the analyses described in this work is publicly available at GitLab (<https://gitlab.com/Biorubens/meta-sci-app>).

Declarations

Ethics approval and consent to participate

Not applicable.

Consent for publication

Not applicable.

Competing interests

The authors declare that they have no competing interests.

Author details

¹Computational Biomedicine Laboratory, Principe Felipe Research Center (CIPF), Valencia 46012, Spain

²Area of Applied Mathematics, Department of Applied Mathematics, Universitat de València, Burjassot 46100, Spain

³Neuronal and Tissue Regeneration Laboratory, Principe Felipe Research Center (CIPF), Valencia 46012, Spain

Received: 28 June 2024 / Accepted: 18 December 2024

Published online: 04 February 2025

References

- Silva NA, Sousa N, Reis RL, Salgado AJ. From basics to clinical: a comprehensive review on spinal cord injury. *Prog Neurobiol.* 2014;114:25–57.
- Kang Y, Ding H, Zhou H, Wei Z, Liu L, Pan D, et al. Epidemiology of worldwide spinal cord injury: a literature review. *J Neurorestoratology.* 2017;6:1–9.
- Ahuja CS, Wilson JR, Nori S, Kotter MRN, Druschel C, Curt A, et al. Traumatic spinal cord injury. *Nat Rev Dis Primer.* 2017;3:17018.
- Courtine G, Sofroniew MV. Spinal cord repair: advances in biology and technology. *Nat Med.* 2019;25:898–908.
- Nas K. Rehabilitation of spinal cord injuries. *World J Orthop.* 2015;6:8.
- Kathe C, Skinnider MA, Hutson TH, Regazzi N, Gautier M, Demesmaeker R, et al. The neurons that restore walking after paralysis. *Nature.* 2022;611:540–7.
- Subramanian A, Tamayo P, Mootha VK, Mukherjee S, Ebert BL, Gillette MA, et al. Gene set enrichment analysis: a knowledge-based approach for interpreting genome-wide expression profiles. *Proc Natl Acad Sci.* 2005;102:15545–50.
- Normand S-LT. Meta-analysis: formulating, evaluating, combining, and reporting. *Stat Med.* 1999;18:321–59.
- Ramirez Flores RO, Lanzer JD, Holland CH, Leuschner F, Most P, Schultz J, et al. Consensus Transcriptional Landscape of Human End-Stage Heart failure. *J Am Heart Assoc.* 2021;10:e019667.
- Barrett T, Wilhite SE, Ledoux P, Evangelista C, Kim IF, Tomashevsky M, et al. NCBI GEO: archive for functional genomics data sets—update. *Nucleic Acids Res.* 2012;41:D991–5.
- Kolesnikov N, Hastings E, Keays M, Melnichuk O, Tang YA, Williams E, et al. ArrayExpress update—simplifying data submissions. *Nucleic Acids Res.* 2015;43:D1113–6.
- Liberati A, Altman DG, Tetzlaff J, Mulrow C, Gøtzsche PC, Ioannidis JPA, et al. The PRISMA Statement for reporting systematic reviews and Meta-analyses of studies that evaluate Health Care interventions: explanation and elaboration. *PLoS Med.* 2009;6:e1000100.
- Mataliotakis GI, Tsirikos AI. Spinal cord trauma: pathophysiology, classification of spinal cord injury syndromes, treatment principles and controversies. *Orthop Trauma.* 2016;30:440–9.
- Kjell J, Olson L. Rat models of spinal cord injury: from pathology to potential therapies. *Dis Model Mech.* 2016;9:1125–37.
- Merle NS, Noe R, Halbwachs-Mecarelli L, Fremeaux-Bacchi V, Roumenina LT. Complement system part II: role in immunity. *Front Immunol.* 2015;6.
- Lubbers R, Van Essen MF, Van Kooten C, Trouw LA. Production of complement components by cells of the immune system. *Clin Exp Immunol.* 2017;188:183–94.
- Alizadeh A, Dyck SM, Karimi-Abdolrezaee S. Traumatic spinal cord injury: an overview of pathophysiology, models and Acute Injury mechanisms. *Front Neurol.* 2019;10:282.
- Di Giovanni S, Knobloch SM, Brandoli C, Aden SA, Hoffman EP, Faden AI. Gene profiling in spinal cord injury shows role of cell cycle in neuronal death. *Ann Neurol.* 2003;53:454–68.
- Wu J, Stoica BA, Faden AI. Cell cycle activation and spinal cord injury. *Neurotherapeutics.* 2011;8:221–8.
- Zhou Y, Wang Z, Li J, Li X, Xiao J. Fibroblast growth factors in the management of spinal cord injury. *J Cell Mol Med.* 2018;22:25–37.
- Kanno H, Pearse DD, Ozawa H, Itoi E, Bunge MB. Schwann cell transplantation for spinal cord injury repair: its significant therapeutic potential and prospectus. *Rev Neurosci.* 2015;26.
- Spann RA, Lawson WJ, Grill RJ, Garrett MR, Grayson BE. Chronic spinal cord changes in a high-fat diet-fed male rat model of thoracic spinal contusion. *Physiol Genomics.* 2017;49:519–29.
- Rabchevsky AG, Michael FM, Patel SP. Mitochondria focused neurotherapeutics for spinal cord injury. *Exp Neurol.* 2020;330:113332.
- Karova K, Wainwright JV, Machova-Urdzikova L, Pisal RV, Schmidt M, Jendelova P, et al. Transplantation of neural precursors generated from spinal progenitor cells reduces inflammation in spinal cord injury via NF- κ B pathway inhibition. *J Neuroinflammation.* 2019;16:12.
- Wang T, Yuan W, Liu Y, Zhang Y, Wang Z, Zhou X, et al. The role of the JAK-STAT pathway in neural stem cells, neural progenitor cells and reactive astrocytes after spinal cord injury. *Biomed Rep.* 2015;3:141–6.
- Satriotomo I, Bowen KK, Vemuganti R. JAK2 and STAT3 activation contributes to neuronal damage following transient focal cerebral ischemia. *J Neurochem.* 2006;98:1353–68.
- Bengochea-Alonso MT, Ericsson J. The phosphorylation-dependent regulation of nuclear SREBP1 during mitosis links lipid metabolism and cell growth. *Cell Cycle.* 2016;15:2753–65.

28. Li C, Wu Z, Zhou L, Shao J, Hu X, Xu W, et al. Temporal and spatial cellular and molecular pathological alterations with single-cell resolution in the adult spinal cord after injury. *Signal Transduct Target Ther*. 2022;7:65.
29. Cao J, Tang T, Tan J, Chen Q, Yuan J, Li T, et al. Expression profiles of long noncoding RNAs and Messenger RNAs in a rat model of spinal cord Injury. *Comput Math Methods Med*. 2023;2023:1–18.
30. Verma R, Viridi JK, Singh N, Jaggi AS. Animals models of spinal cord contusion injury. *Korean J Pain*. 2019;32:12.
31. Khuyagbaatar B, Kim K, Kim YH. Conversion equation between the Drop Height in the New York University Impactor and the Impact Force in the infinite Horizon Impactor in the Contusion spinal cord Injury Model. *J Neurotrauma*. 2015;32:1987–93.
32. Kyritsis N, Torres-Espin A, Schupp PG, Huie JR, Chou A, Duong-Fernandez X, et al. Diagnostic blood RNA profiles for human acute spinal cord injury. *J Exp Med*. 2021;218:e20201795.
33. Roberts TT, Leonard GR, Cepela DJ. Classifications in brief: American Spinal Injury Association (ASIA) impairment scale. *Clin Orthop*. 2017;475:1499–504.
34. Merikangas AK, Shelly M, Knighton A, Kotler N, Tanenbaum N, Almsay L. What genes are differentially expressed in individuals with schizophrenia? A systematic review. *Mol Psychiatry*. 2022;27:1373–83.
35. Squair JW, Tigchelaar S, Moon K-M, Liu J, Tetzlaff W, Kwon BK, et al. Integrated systems analysis reveals conserved gene networks underlying response to spinal cord injury. *eLife*. 2018;7:e39188.
36. Wilkinson MD, Dumontier M, Aalbersberg IJ, Appleton G, Axton M, Baak A, et al. The FAIR Guiding principles for scientific data management and stewardship. *Sci Data*. 2016;3:160018.
37. Tica J, Bradbury E, Didangelos A. Combined transcriptomics, proteomics and Bioinformatics identify drug targets in spinal cord Injury. *Int J Mol Sci*. 2018;19:1461.
38. Haggerty AE, Marlow MM, Oudega M. Extracellular matrix components as therapeutics for spinal cord injury. *Neurosci Lett*. 2017;652:50–5.
39. De Castro R, Burns CL, McAdoo DJ, Romanic AM. Metalloproteinase increases in the injured rat spinal cord. *NeuroReport*. 2000;11:3551–4. <https://doi.org/10.1097/00001756-200011090-00029>. PMID: 11095516.
40. Albayar AA, Roche A, Swiatkowski P, Antar S, Ouda N, Emara E, et al. Biomarkers in spinal cord Injury: prognostic insights and future potentials. *Front Neurol*. 2019;10:27.
41. Kwon BK, Casha S, Hurlbert RJ, Yong VW. Inflammatory and structural biomarkers in acute traumatic spinal cord injury. *cclm*. 2011;49:425–33.
42. Rosell A, Cuadrado E, Ortega-Aznar A, Hernández-Guillamon M, Lo EH, Montaner J. MMP-9-Positive neutrophil infiltration is Associated to blood-brain barrier breakdown and basal Lamina type IV collagen degradation during Hemorrhagic Transformation after Human ischemic stroke. *Stroke*. 2008;39:1121–6.
43. Zhang S-X, Underwood M, Landfield A, Huang F, Gibson S, Geddes JW. Cytoskeletal Disruption Following Contusion Injury to the rat spinal cord. *J Neuropathol Exp Neurol*. 2000;59:287–96.
44. Wu J, Stoica BA, Dinizo M, Pajoohesh-Ganji A, Piao C, Faden AI. Delayed cell cycle pathway modulation facilitates recovery after spinal cord injury. *Cell Cycle*. 2012;11:1782–95.
45. Di Giovanni S, Movsesyan V, Ahmed F, Cernak I, Schinelli S, Stoica B, et al. Cell cycle inhibition provides neuroprotection and reduces glial proliferation and scar formation after traumatic brain injury. *Proc Natl Acad Sci*. 2005;102:8333–8.
46. Kabadi SV, Stoica BA, Byrnes KR, Hanscom M, Loane DJ, Faden AI. Selective CDK inhibitor limits Neuroinflammation and Progressive Neurodegeneration after Brain Trauma. *J Cereb Blood Flow Metab*. 2012;32:137–49.
47. Skovira JW, Wu J, Matyas JJ, Kumar A, Hanscom M, Kabadi SV, et al. Cell cycle inhibition reduces inflammatory responses, neuronal loss, and cognitive deficits induced by hypobaric exposure following traumatic brain injury. *J Neuroinflammation*. 2016;13:299.
48. Milich LM, Ryan CB, Lee JK. The origin, fate, and contribution of macrophages to spinal cord injury pathology. *Acta Neuropathol (Berl)*. 2019;137:785–97.
49. Kopper TJ, Gensel JC. Myelin as an inflammatory mediator: myelin interactions with complement, macrophages, and microglia in spinal cord injury. *J Neurosci Res*. 2018;96:969–77.
50. Chamankhah M, Eftekharpour E, Karimi-Abdolrezaee S, Boutros PC, San-Marina S, Fehlings MG. Genome-wide gene expression profiling of stress response in a spinal cord clip compression injury model. *BMC Genomics*. 2013;14:583.
51. Gaudet AD, Popovich PG. Extracellular matrix regulation of inflammation in the healthy and injured spinal cord. *Exp Neurol*. 2014;258:24–34.
52. Piro RM, Ala U, Molineris I, Grassi E, Bracco C, Perego GP, et al. An atlas of tissue-specific conserved coexpression for functional annotation and disease gene prediction. *Eur J Hum Genet*. 2011;19:1173–80.
53. Pierson E, the GTEx Consortium, Koller D, Battle A, Mostafavi S. Sharing and specificity of co-expression networks across 35 human tissues. *PLOS Comput Biol*. 2015;11:e1004220.
54. De Biase A, Knoblauch SM, Di Giovanni S, Fan C, Molon A, Hoffman EP, et al. Gene expression profiling of experimental traumatic spinal cord injury as a function of distance from impact site and injury severity. *Physiol Genomics*. 2005;22:368–81.
55. Sueda R, Imayoshi I, Harima Y, Kageyama R. High Hes1 expression and resultant Ascl1 suppression regulate quiescent vs. active neural stem cells in the adult mouse brain. *Genes Dev*. 2019;33:511–23.
56. Wang X, Wang Q, Tian H, Lv W, Song L, Li Z, et al. Electroacupuncture in promoting neural repair after spinal cord injury: inhibiting the notch signaling pathway and regulating downstream proteins expression. *Anat Rec*. 2021;304:2494–505.
57. Ruan W, Ning G, Feng S, Gao S, Hao Y. MicroRNA-381/Hes1 is a potential therapeutic target for spinal cord injury. *Int J Mol Med*. 2018. <https://doi.org/10.3892/ijmm.2018.3658>.
58. Kabayiza KU, Masgutova G, Harris A, Rucchin V, Jacob B, Clotman F. The Onecut transcription factors regulate differentiation and distribution of dorsal interneurons during spinal Cord Development. *Front Mol Neurosci*. 2017;10:157.
59. Roy A, Francius C, Rousso DL, Seuntjens E, Debruyjn J, Luxenhofer G, et al. Onecut transcription factors act upstream of *Isl1* to regulate spinal motoneuron diversification. *Development*. 2012;139:3109–19.
60. Toch M, Harris A, Schakman O, Kondratskaya E, Boulland J-L, Dauguet N, et al. Onecut-dependent Nkx6.2 transcription factor expression is required for proper formation and activity of spinal locomotor circuits. *Sci Rep*. 2020;10:996.
61. Chevreau R, Ghazale H, Ripoll C, Chalfouh C, Delarue Q, Hemonnot-Girard AL, et al. RNA profiling of Mouse Ependymal Cells after spinal cord Injury identifies the Oncostatin Pathway as a potential Key Regulator of spinal cord stem cell fate. *Cells*. 2021;10:3332.
62. Wang S-M, Hsu J-YC, Ko C-Y, Chiu N-E, Kan W-M, Lai M-D, et al. Astrocytic CCAAT/Enhancer-Binding Protein Delta Contributes to glial scar formation and impairs functional recovery after spinal cord Injury. *Mol Neurobiol*. 2016;53:5912–27.
63. Raivich G, Bohatschek M, Da Costa C, Iwata O, Galiano M, Hristova M, et al. The AP-1 transcription factor c-Jun is required for efficient axonal regeneration. *Neuron*. 2004;43:57–67.
64. Zhang T, Gao G, Chang F. miR-152 promotes spinal cord injury recovery via c-jun amino terminal kinase pathway. *Eur Rev Med Pharmacol Sci*. 2019;23:44–51.
65. Nagano S, Kim SH, Tokunaga S, Arai K, Fujiki M, Misumi K. Matrix metalloproteinase-9 activity in the cerebrospinal fluid and spinal injury severity in dogs with intervertebral disc herniation. *Res Vet Sci*. 2011;91:482–5.
66. Qi D, Geng Y, Cardenas J, Gu J, Yi SS, Huang JH, et al. Transcriptomic analyses of patient peripheral blood with hemoglobin depletion reveal glioblastoma biomarkers. *Npj Genomic Med*. 2023;8:2.
67. Ritchie ME, Phipson B, Wu D, Hu Y, Law CW, Shi W, et al. Limma powers differential expression analyses for RNA-sequencing and microarray studies. *Nucleic Acids Res*. 2015;43:e47–47.
68. Benjamini Y, Hochberg Y. Controlling the false Discovery rate: a practical and powerful Approach to multiple testing. *J R Stat Soc Ser B Methodol*. 1995;57:289–300.
69. DerSimonian R, Laird N. Meta-analysis in clinical trials. *Control Clin Trials*. 1986;7:177–88.
70. Viechtbauer W. Conducting Meta-analyses in R with the metafor Package. *J Stat Softw*. 2010;36.
71. Rohart F, Gautier B, Singh A, Lê Cao K-A, mixOmics. An R package for 'omics feature selection and multiple data integration. *PLOS Comput Biol*. 2017;13:e1005752.
72. Montaner D, Dopazo J. Multidimensional gene set analysis of genomic data. *PLoS ONE*. 2010;5:e10348.
73. Ashburner M, Ball CA, Blake JA, Botstein D, Butler H, Cherry JM, et al. Gene Ontology: tool for the unification of biology. *Nat Genet*. 2000;25:25–9.
74. Kanehisa M. The KEGG resource for deciphering the genome. *Nucleic Acids Res*. 2004;32:D277–280.

75. Vastrik I, D'Eustachio P, Schmidt E, Joshi-Tope G, Gopinath G, Croft D, et al. Reactome: a knowledge base of biologic pathways and processes. *Genome Biol.* 2007;8:R39.
76. Alvarez MJ, Shen Y, Giorgi FM, Lachmann A, Ding BB, Ye BH, et al. Functional characterization of somatic mutations in cancer using network-based inference of protein activity. *Nat Genet.* 2016;48:838–47.
77. Garcia-Alonso L, Holland CH, Ibrahim MM, Turei D, Saez-Rodriguez J. Benchmark and integration of resources for the estimation of human transcription factor activities. *Genome Res.* 2019;29:1363–75.
78. Abu-Jamous B, Kelly S. Clust: automatic extraction of optimal co-expressed gene clusters from gene expression data. *Genome Biol.* 2018;19:172.
79. Szklarczyk D, Gable AL, Nastou KC, Lyon D, Kirsch R, Pyysalo S, et al. The STRING database in 2021: customizable protein–protein networks, and functional characterization of user-uploaded gene/measurement sets. *Nucleic Acids Res.* 2021;49:D605–12.
80. Beatriz, Martínez-Rojas Esther, Giraldo Rubén, Grillo-Risco Marta R., Hidalgo Eric, López-Mocholi Ana, Alastrue-Agudo Francisco, García-García Victoria, Moreno-Manzano. NPC transplantation rescues sci-driven cAMP/EPAC2 alterations leading to neuroprotection and microglial modulation. *Cell Mol Life Sci.* 2022;79(8) . <https://doi.org/10.1007/s00018-022-04494-w>.

Publisher's note

Springer Nature remains neutral with regard to jurisdictional claims in published maps and institutional affiliations.